Article

Street Centralities and Land Use Intensities Based on Points of Interest (POI) in Shenzhen, China

Shuai Wang [1], **Gang Xu [1],*** and **Qingsheng Guo [1,2],***

[1] School of Resource and Environmental Sciences, Wuhan University, Wuhan 430079, China; 2010282050194@whu.edu.cn

[2] State Key Laboratory of Information Engineering in Surveying, Mapping and Remote Sensing, Wuhan University, Wuhan 430079, China

* Correspondence: xugang@whu.edu.cn (G.X); guoqingsheng@whu.edu.cn (Q.G.); Tel.: +86-27-6877-8381 (G.X. & Q.G.)

check for
updates

Abstract: Urban land use and transportation are closely associated. Previous studies have investigated the spatial interrelationship between street centralities and land use intensities using land cover data, thus neglecting the social functions of urban land. Taking the city of Shenzhen, China, as a case study, we used reclassified points of interest (POI) data to represent commercial, public service, and residential land, and then investigated the varying interrelationships between the street centralities and different types of urban land use intensities. We calculated three global centralities ("closeness", "betweenness", and "straightness") as well as local centralities (1-km, 2-km, 3-km, and 5-km searching radiuses), which were transformed into raster frameworks using kernel density estimation (KDE) for correlation analysis. Global closeness and straightness are high in the urban core area, and roads with high global betweenness outline the skeleton of the street network. The spatial patterns of the local centralities are distinguished from the global centralities, reflecting local location advantages. High intensities of commercial and public service land are concentrated in the urban core, while residential land is relatively scattered. The bivariate correlation analysis implies that commercial and public service land are more dependent on centralities than residential land. Closeness and straightness have stronger abilities in measuring the location advantages than betweenness. The centralities and intensities are more positively correlated on a larger scale (census block). These findings of the spatial patterns and interrelationships of the centralities and intensities have major implications for urban land use and transportation planning.

Keywords: street network; land use intensity; street centralities; POI; complex network

1. Introduction

Urban land use and transportation are two crucial subsystems within urban systems that mutually interact and influence each other [1–4]. Urban roads facilitate socioeconomic activities taking place on urban land, and urban land use, in turn, influences the travel behavior of citizens [5–7]. Urban socioeconomic activities and land use are never evenly distributed in self-organized cities nor planned cities, and urban roads are the same. Therefore, the spatial correlation between urban land use and urban roads has long been a major research interest of urban researchers and planners [8–10].

Street networks, composed of urban roads, are called the skeleton of a city [11]. A street network is a typical complex network with two different representations, duel representation and primal representation, which can be characterized and quantified by metrics and topological measurements [12,13]. Centrality is a fundamental concept in graph theory and network science, which identifies the most important vertices within a graph, for instance, the key infrastructure nodes in

urban street networks [14,15]. Street centrality captures location advantages in a city and plays a crucial role in shaping the intraurban variation of urban structures and land uses [16]. Previous studies have examined the interrelationship between different centrality indicators ("betweenness", "closeness", and "straightness") and economic activities or general land uses intensities within a city [17–19]. For example, Wang et al. [16] analyzed the relationship between street centralities and land use intensities, which are represented by population densities and employment densities. We seek to further understand how street centralities specifically influence different types of urban land use, such as commercial land, residential land, and industrial land.

However, to the best of our knowledge, there are few studies focusing on the influence of centrality indicators on different types of urban land use. Rui and Ban (2014) found variant correlations between different centralities and land use types in Stockholm using land-cover data [20]. Chaudhuri and Clarke [21] used land-cover data (urban areas, natural areas, agricultural land use, and water bodies) to investigate the spatiotemporal dynamics of the coupling between land use (change) and street networks. However, land cover data can only quantify the spatial extent of land use and cannot characterize the intensity of land use. Urban land use can be differentiated either by their physical properties or social functions [22,23]. Remote sensing has long been used to acquire the physical properties of land use and to classify land into land cover types [24], which neglects knowing the social functions of urban land use [22]. Emerging types of big data, such as mobile phone data, points of interest (POI), trajectories, and social media data, have been used to acquire fine urban land use classifications [22,25–31], providing solutions for acquiring different types of urban land use.

A point of interest (POI) is a specific point location, referring to all geographical entities that can be abstracted as points. Previous studies have suggested that POI data is capable of describing land use at a disaggregated level and has a finer grain than a conventional land use map [32]. Using POI data can not only identify the types of urban land use, but also their intensities. In this study, taking the city of Shenzhen, China, as a case study, we use points of interest (POI) to represent different urban land use types and their intensities, namely, commercial land, public service land, and residential land. We focus on the distinguished interrelationships between street centralities and different urban land use intensities.

2. Study Area and Data

2.1. Study Area

Shenzhen, located in the south of China, is one of the youngest megacities in China (Figure 1). Thanks to China's Open Policy reform, Shenzhen has experienced rapid growth over the past few decades. In 2016, the permanent resident population in Shenzhen was 12 million, with a gross domestic product (GDP) of approximately 300 billion USD [33]. There are ten districts in Shenzhen, namely: Luohu, Futian, Nanshan, Yantian, Baoan, Longgang, Longhua, Guangming, Pingshan, and Dapeng (Figure 1), among which Luohu, Futian, Nanshan, and Yantian are the four initial special economic zones in Shenzhen [34]. Presently, Futian and Luohu are the downtown areas and Nanshan is the high-technology zone in Shenzhen City [35].

Shenzhen is not built on China's vast plains, but instead around hills along the coastline (Figure 1). Restricted by its special terrain, Shenzhen implemented a multicluster urban master plan at the beginning of its establishment [32,35]. In each urban cluster, planners have assigned and designed employment and residential areas to minimize commuting across clusters. Under such circumstances, the roads carrying commuting across clusters are particularly important in the street network.
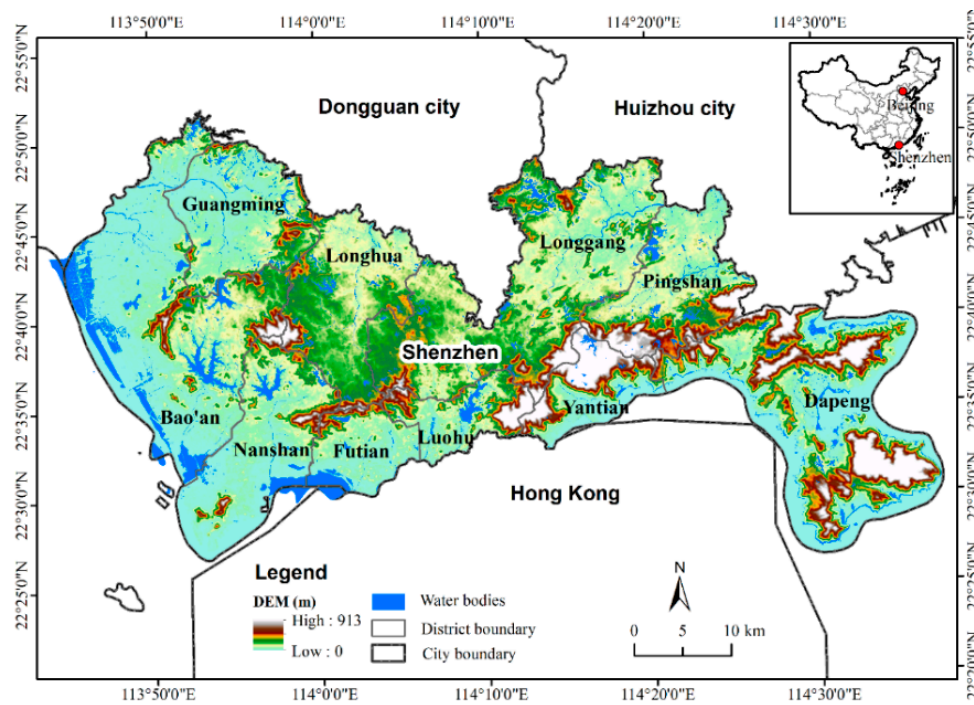
Figure 1. Location of Shenzhen City in China and its spatial extent.

2.2. Street Network

Street centralities' characterization heavily relies on the high-quality data of urban roads. OpenStreetMap, which uses edits and updates of roads across the world done by volunteers, can be a vital approach for acquiring urban roads, and has been successfully used in other studies [36–40]. Nevertheless, there are two obstacles (typology and file format) in building a street network using OpenStreetMap road data. Recently, Boeing has developed a useful toolbox (OSMnx) based on Python programming, which can easily download a street network from OpenStreetMap, check and correct the network topology, and analyze the street networks [38]. Specifically, this toolbox produces nodes only at locations where roads intersect, thus excluding overpasses and tunnels. This process results in a nonplanar graph, while most of the previous studies simplify the street networks as planar networks [38].

We used OSMnx to download the drivable urban roads in Shenzhen City on 8 February 2018 [38]. There are 28,064 nodes (intersections) and 41,789 edges (links between two intersections) in the street network. The road length (length of edges) and kernel density of the nodes (using kernel density estimation (KDE) in a default searching radius) are presented in Figure 2a,b, respectively. The road length varies from 0.2 m to 13.6 km, with a mean of 223.1 m. The total length of the roads is 9323 km, and the average road density in Shenzhen is 4.67 km/km^2 (the land area in Shenzhen City is 1997 km^2). The length of the edges is relatively short in the core area, while long edges are roads across districts (Figure 2a). A high density of nodes are concentrated in the core area (Futian, Nanshan, and Luohu districts) (Figure 2b). In the following section, we analyzed the correlation between the street centralities and land use intensities in Shenzhen, excluding the Dapeng district, because of the sparse roads there (Figure 2a).
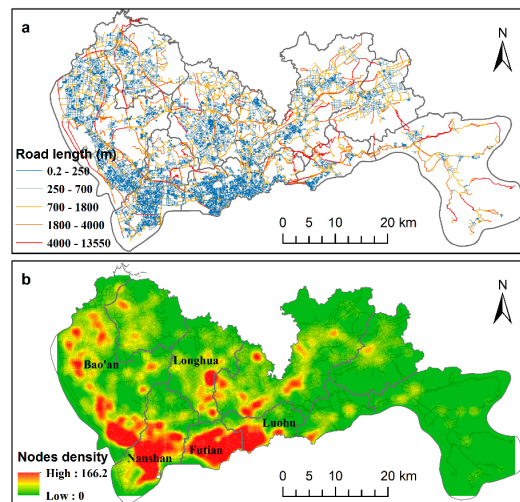
Figure 2. Spatial distribution of the road net and road lengths in Shenzhen City (**a**) and density of nodes in Shenzhen City (**b**). The nodes density used the kernel density estimation (KDE) in a default searching radius.

2.3. Points of Interest (POI)

We collected the POI data in Shenzhen City from Amap (https://www.amap.com/) on 28 February 2018, with a total of 611,122 records. These POIs are divided into 15 primary categories and 81 subcategories. The numbers and proportions of POIs in the 15 primary categories are presented in Figure 3. The core function of a city is to provide urban residents with housing and employment, as well as public services. On the other hand, from the perspective of urban land functions, the most important land types are commercial land, residential land, and industrial land. Unfortunately, the POI data we obtained cannot accurately identify the industrial land in Shenzhen City (Figure 3). Therefore, we summarized the POI data into three categories, namely, commercial and business facilities, residential sites, and administration and public services (see detailed information in Figure 3). We used the three categories of POIs to represent commercial land, residential land, and public service land, respectively (Figure 3).
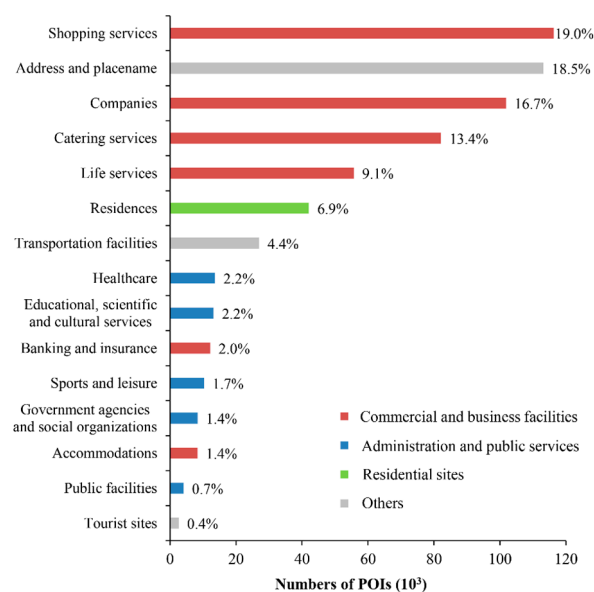
Figure 3. Numbers and proportions of 15 primary categories of points of interest (POIs) in Shenzhen City. These POIs are divided into commercial and business facilities (61.6%), residential sites (6.9%), administration and public services (8.1%), and others (23.4%).

3. Methods

3.1. Street Centrality Measures

Centrality plays a crucial role in understanding the structural properties of the complex relational network [15]. The multiple centrality assessment (MCA) method has been broadly used to analyze urban street networks based on primal graphs, in which the road intersections are turned into nodes, and the connections between the nodes have been turned into edges [16,18,19,41]. There are three centrality indicators, namely, the closeness centrality, betweenness centrality, and straightness centrality, which have been widely used in related studies [16,18–20].

Closeness centrality (C^C) quantifies to what extent a node (i) is close to all of the other nodes along the shortest paths of the network, which is defined as follows:

$$C_i^C = \frac{N-1}{\sum\limits_{i=1;j\neq 1}^{N} d_{ij}} \tag{1}$$

where N is the total number of nodes in the network and d_{ij} is the shortest path length between node i and j.

Betweenness centrality (C^B) quantifies the centrality of a node (i) by counting how many times the node (i) is traversed by the shortest paths of all of the pairs of nodes in the network, which is defined as follows:

$$C_i^B = \frac{1}{(N-1)(N-2)} \sum_{\substack{j=1;k=1;\\ j\neq k\neq i}}^{N} \frac{n_{jk}(i)}{n_{jk}} \tag{2}$$

where n_{jk} is the number of shortest paths between nodes j and k, and $n_{jk}(i)$ is the number of these shortest paths that traverse node i.

Straightness centrality (C^S) quantifies the extent of a deviation of the distance from the shortest path and the straight line between node i and j, which is defined as follows:

$$C_i^S = \frac{1}{N-1} \sum_{j=1;j\neq k}^{N} \frac{d_{ij}^{Eucl}}{d_{ij}} \tag{3}$$

where d^{Eucl}_{ij} is the Euclidean distance between node i and j. A higher straightness centrality (C^s) of node (i) means a better directness to the node, resulting a higher commuting efficiency.

We calculated these centrality indicators at each node using urban network analysis tools [41], which can be executed as a toolbox in a GIS software. The centrality indicator of a node is largely affected by the searching radius. The default searching radius is infinite, and when calculating a node's centrality indicator, the arithmetic will traverse all of the nodes in the road network, resulting in global centralities. Local centralities with specific searching radiuses (1 km, 2 km, 3 km, and 5 km) are also calculated, which will be presented in the discussion section.

3.2. Kernel Density Estimation (KDE)

As the calculation of street centralities is based on nodes (points), and POI data is also the point data, which are unevenly distributed, we need centralities and land use intensities across the whole study area in order to perform a correlation analysis. Among the numerous methods of spatial smoothing and spatial interpolation, kernel density estimation (KDE) has been commonly used to transform the results of street centralities and land use intensities into continuous raster frameworks [17,18]. KDE is a nonparametric way to estimate the probability density function of a random variable. In GIS, KDE uses the density within a range (window) of each observation in order

to calculate the value at the center of the window by weighting nearby observations more than distant observations based on a kernel function [17]. The definition of the equation and a detailed explanation of KDE can be found in a previous relevant paper [17].

We used KDE to acquire the raster frameworks of the centrality indicators and POI-based urban land use intensities. We first used the default searching radius of the KDE method in ArcGIS10.2, which is the shortest of the width or height of the output extent in the output spatial reference divided by 30. In this study, the searching radius in KDE ranges from 1145 m (for commercial and business facilities) to 1400 m (for residential sites). We calculated the urban land use intensities under different searching radiuses in KDE (1 km, 2 km, 3 km, and 5 km). The centrality indicators and land use intensities under different searching radiuses in KDE are highly correlated. Thus, we only compare the correlations between the centrality indicators and land use intensities using the raster frameworks under the default searching radius in KDE. The use of the default searching radius in KDE is to avoid any confusion with the searching radiuses in the calculation of the local centralities. The cell size for the output raster dataset is defined as the default value in ArcGIS10.2, which is the shorter of the width or height of the output extent in the output spatial reference divided by 250. In this study, the height of the output extent is shorter, which is approximately 45 km, resulting in a cell size of approximately 180 m.

After acquiring raster frameworks, we used the 1 km grid and subdistricts (census blocks) in Shenzhen to summarize the centrality indicators and land use intensities. Then, we used the Pearson's correlation analysis to investigate the correlation between the street centralities and land use intensities. We first presented the results of correlation analysis using a 1 km grid ($N = 1621$), and we compared that with the correlation results using census blocks ($N = 58$) in order to check the influences of the units in the correlation analysis. The overall flowchart of this study is shown in Figure 4.
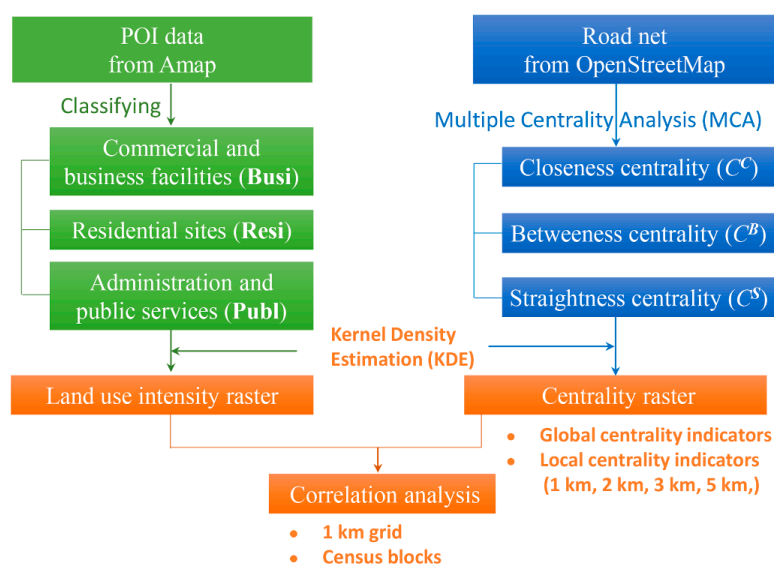

Figure 4. Flowchart of analysis of interrelationship between street centralities and POI-based urban land use intensities.

4. Results

4.1. Spatial Patterns of Street Centralities

We first calculated three global centrality indicators at each node using urban network analysis tools [41]. Then, the centralities of the edges are summarized using the average of the centralities of the two nodes linking to this edge [16]. The spatial distributions of the three centrality indicators using KDE in the default searching radiuses are presented in Figure 5. The frequency distributions of the three centralities indicators at the node level are presented in Figure 6.
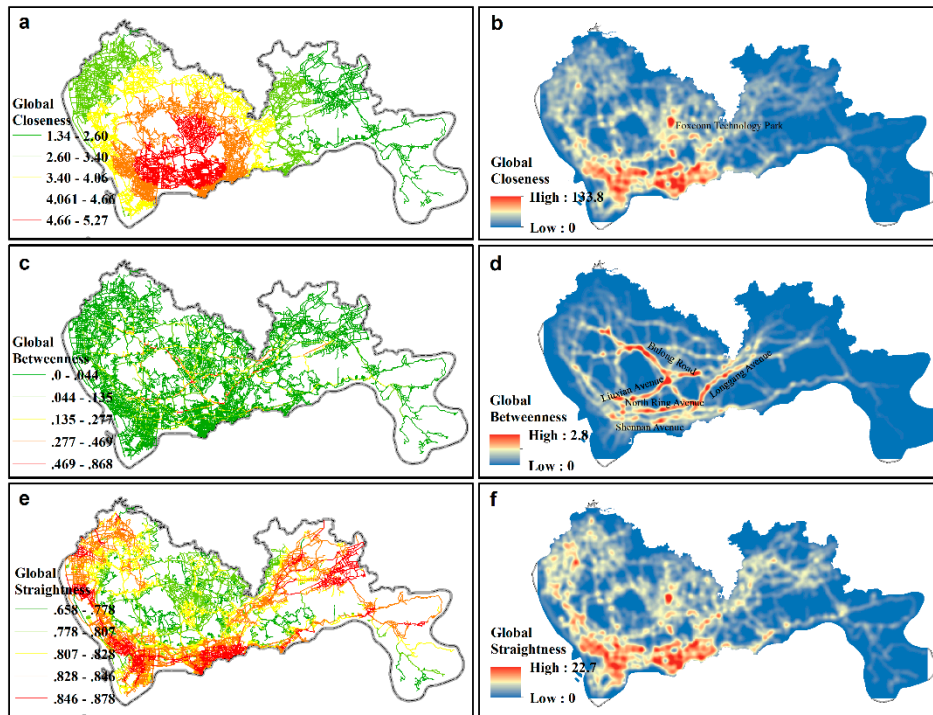
Figure 5. Spatial distributions of global centrality indicators of street networks in Shenzhen. The centrality indicators of each edge are averaged from two nodes linking to this edge, and they are divided into five levels using natural breaks in ArcGIS10.2 (**a,c,e**); kernel density estimation of centrality indicators at nodes (**b,d,f**).
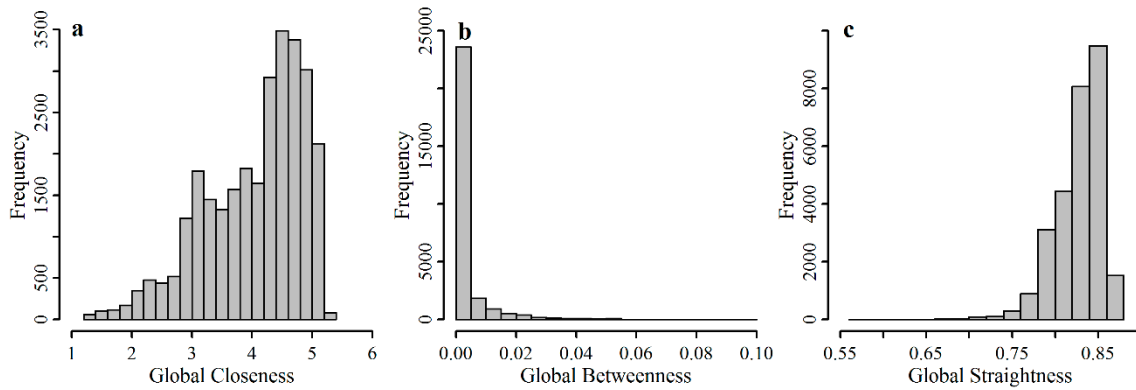
Figure 6. Frequency distribution of global centrality indicators at each node, global closeness (**a**), global betweenness (**b**), and global straightness (**c**).

Global closeness centrality (Glob C^C) presents a concentric ring form, which decreases from the center to the outside (Figure 5a). The highest value of Glob C^C in the core area reflects the location advantage within the whole network (Figure 5a). The results of KDE show that high values of Glob C^C are concentrated in the urban core area, namely, the Futian, Luohu, and Nanshan Districts (Figure 5b). In Longhua District, which is relatively far from the urban core area, there is also a high-value area of Glob C^C. This is the Foxconn Technology Park, where urban roads are dense and have a high Glob C^c (Figure 5b).

The spatial patterns of global betweenness centralities (Glob C^B) are obviously different from those of Glob C^C. Most of the roads show a very low Glob C^B (Figures 5c and 6b), and only important roads have a high Glob C^B, which can be more clearly seen in the KDE results (Figure 5d). Shennan Avenue and North Ring Avenue are the east–west arteries, playing an important role in connection within the core urban area; thus, the two roads present a high Glob C^B. Other highways or expressways

connecting different urban clusters also have a high Glob C^B. Those roads with a low Glob C^B are not predominant in the whole network, but they could have important connections in the local areas. This dynamic will be reflected in the local centralities.

Global straightness centralities (Glob C^S) are high in the core urban area and in the northeast and west of the city. The typical road length in the urban core areas is short, partly resulting in the relatively high Glob C^S. In contrast to the frequency distribution of Glob C^B, more nodes have a higher Glob C^S (Figure 6b,c). The KDE result shows that a high Glob C^S is concentrated in the core urban area, similar to the spatial pattern of Glob C^C.

4.2. Spatial Distributions of Urban Land Use Intensities

We used the reclassified POI data to represent the following three types of urban land use: commercial land, public service land, and residential land. We used KDE to generate the land use intensity raster frameworks shown in Figure 7. The frequency distributions of land use intensities in a 1 km grid are shown in Figure 8.

Compared to the spatial patterns of the centrality indicators, high intensities of urban land use are more concentrated in smaller areas (Figure 7). Specific to the three types of POI-based urban land use intensities, there are also apparent disparities in their spatial patterns. The intensities of commercial land and public services land are extremely concentrated in the following two urban areas: the Luohu–Futian area and Nanshan–Baoan area (Figure 7a,b). In contrast, the agglomeration of residential land is not as obvious as the other two, and its spatial distribution is relatively scattered. In addition to the centralized distribution of residential land in the core urban area, Longhua and Longgang, which are relatively far from the core urban area, also have a large amount of residential land (Figure 7c).
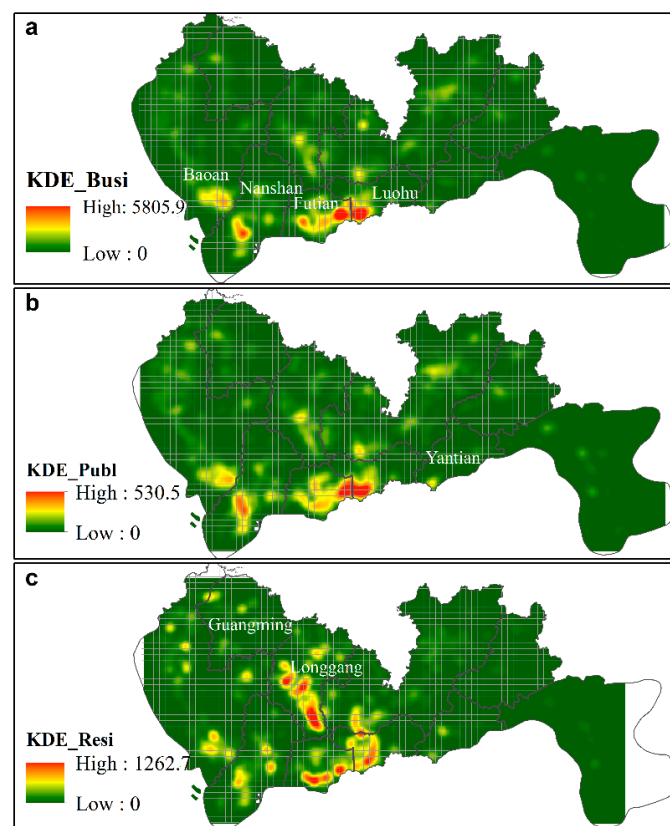

Figure 7. Spatial distributions of intensities of commercial and business facilities (**a**), public and administrative services (**b**), and residential sites (**c**). These represent commercial land use intensities, public service land use intensities, and residential land use intensities, respectively.
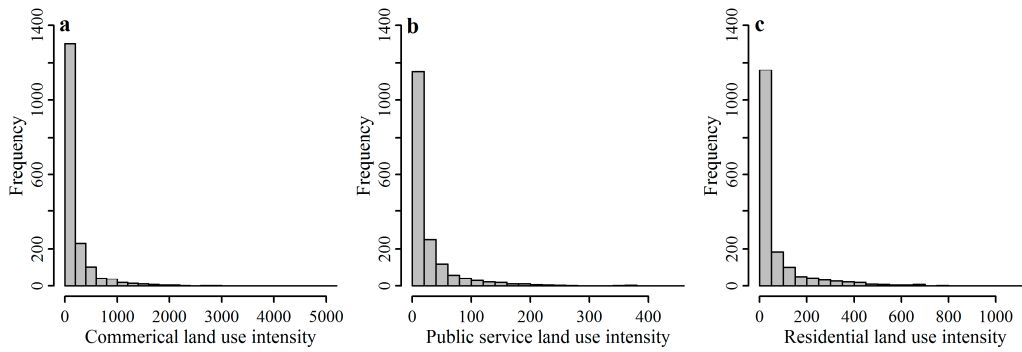
Figure 8. Frequency distributions of land use intensities using kernel density estimation (KDE) in a 1 km grid. (**a**) Commercial land use intensity, (**b**) public service land use intensity, (**c**) residential land use intensity.

4.3. Correlations between Street Centrality and Land Use Intensity

We summarized the street centralities and land use intensities in each 1 km grid. Scatter plots of street centralities and land use intensities excluding the grids with zero values of centralities or intensities are presented in Figure 9. The straight line is the linear regression line between the street centralities and land use intensities. Overall, the street centralities and land use intensities are positively correlated. We used a bivariate correlation analysis (Pearson's *r*) to test the degree of correlation between the street centralities and land use intensities using SPSS 21. We also calculated the Pearson's *r* of the logarithmic form of centralities or land use intensities. The results of the bivariate correlation analysis are presented in Table 1.
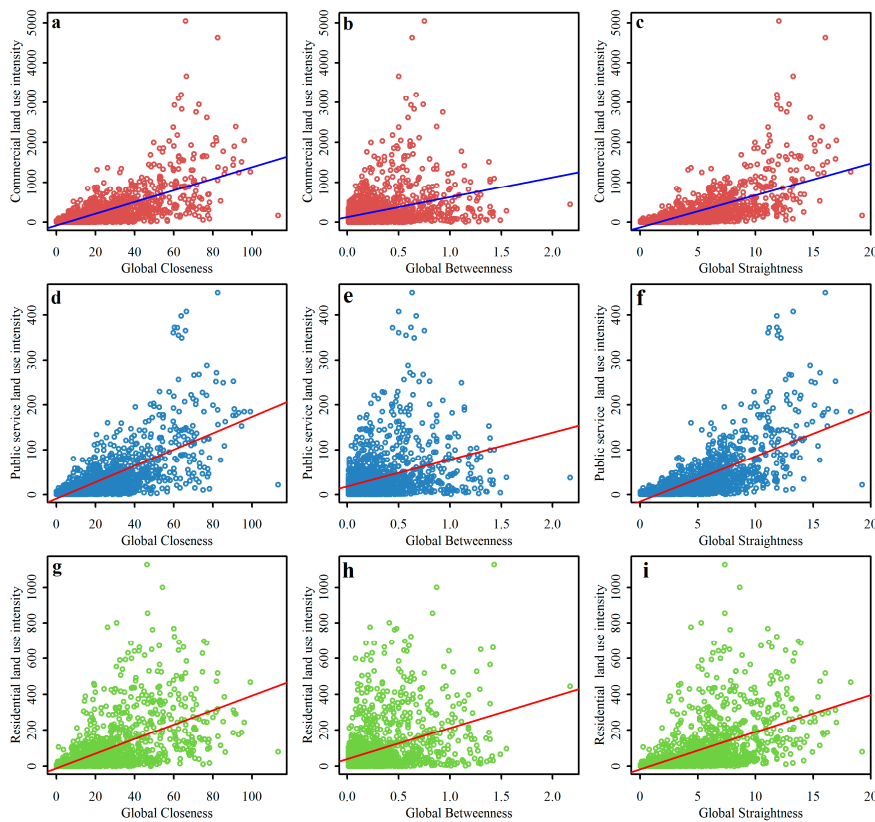
Figure 9. Scatter plots of street centralities and land use intensities. The same vertical column shares the same centrality indicator: Closeness, Betweenness, and Straightness, from left to right, respectively. The same horizontal row shares the same land use intensity: commercial land, public service land, and residential land, from top to bottom, respectively. The straight lines are linear regression lines.

Table 1. Pearson's r between global street centralities and land use intensities in a 1 km grid.

Centralities	Comm #	Publ #	Resi #	Ln(Comm)	Ln(Publ)	Ln(Resi)
Glob C^C	0.670 **	0.701 **	0.585 **	0.679 **	0.677 **	0.648 **
Glob C^B	0.343 **	0.350 **	0.381 **	0.386 **	0.374 **	0.391 **
Glob C^S	0.665 **	0.700 **	0.540 **	0.733 **	0.729 **	0.668 **
Ln(Glob C^C)	0.428 **	0.463 **	0.428 **	0.737 **	0.725 **	0.694 **
Ln(Glob C^B)	0.360 **	0.375 **	0.381 **	0.456 **	0.441 **	0.447 **
Ln(Glob C^S)	0.426 **	0.461 **	0.400 **	0.753 **	0.738 **	0.684 **

\# Comm, Publ, and Resi mean commercial land, public service land, and residential land, respectively. ** $p < 0.01$.

Generally, the street centralities and land use intensities are significantly correlated in all four forms ($x{\sim}y$, Ln$x{\sim}y$, $x{\sim}$Lny, and Ln$x{\sim}$Lny), and their logarithmic forms (Ln$x{\sim}$Lny) show the highest correlation (Table 1). The street centralities have varying impacts on the different types of urban land use. From the perspective of centralities, Glob C^C and Glob C^S have a higher Pearson's r with land use intensities than that of Glob C^B, which implies that the intensities of urban land use are more dependent on the Glob C^C and Glob C^S of the street network. As previously mentioned, Glob C^B measures the nodes that play key roles in connecting the entire street network, and the nodes with an important connectivity may not be active places for socioeconomic activities, which leads to the relatively low correlation between the Glob C^B and urban land use intensities.

In terms of different urban land use, commercial land and public service land have higher Pearson's r values with centralities than that of residential land. Compared with the centralized distribution of commercial land and public service land, the spatial distribution of residential land is scattered, resulting in a lower correlation with street centralities.

5. Discussion

5.1. Local Street Centralities

To test the correlation between the local street centralities and the land use intensities, we calculated three centrality indicators for each code under different searching radiuses of 1 km, 2 km, 3 km, and 5 km. The spatial distributions of the KDE of the local centralities are presented in Figure 10. Generally, the spatial patterns of the local centralities are different from those of the global centralities. The local centralities show the location advantage of the nodes within a local area. In particular, the local C^B measures the connectivity of a road within a local area, whose spatial patterns are more scattered compared to global C^B. The high values of local C^C and local C^S are mainly concentrated in the core area, but there are also obvious locally high values far from the core area (Figure 10). With the increase in the searching radius in the centralities calculations, the spatial pattern of the centralities is closer to the global centralities pattern, thus showing a transformation of local characteristics to the overall features.

We also summarized the local street centralities in the 1 km grid and analyzed their correlations between the local centralities under different searching radiuses and urban land use intensities. Due to the similar degree of correlation in the different forms (Table 1), we only tested the linear correlation between the local centralities and intensities in this study (Table 2). The linear correlation coefficients between the global centralities and land use intensities are also included in Table 2 for comparison. The correlations between local C^C (local C^B) and the land use intensities show a decreasing trend as the searching radius increases from 1 km to 5 km, while the correlations between local C^S and the land use intensities tend to increase as the searching radius increases (Table 2).

In comparisons of the global and local centralities, local C^C_{1km} is more correlated with the intensities of the commercial land and public service land than global C^C, but it is opposite for the residential land. Global C^B has a higher correlation with land use intensities, indicating the higher impact on the urban land use intensities compared to local C^B. However, local C^S has a higher

correlation with urban land use intensities. In summary, the optimal scales of correlation between the commercial land and the three centralities are local C^C_{1km}, global C^B, and local C^S_{5km}, which are shared by public service land. The optimal scales of correlation between the residential land and the three centralities are global C^C, global C^B, and local C^S_{5km}. These Pearson's *r* values under the optimal scales are in bold in Table 2.
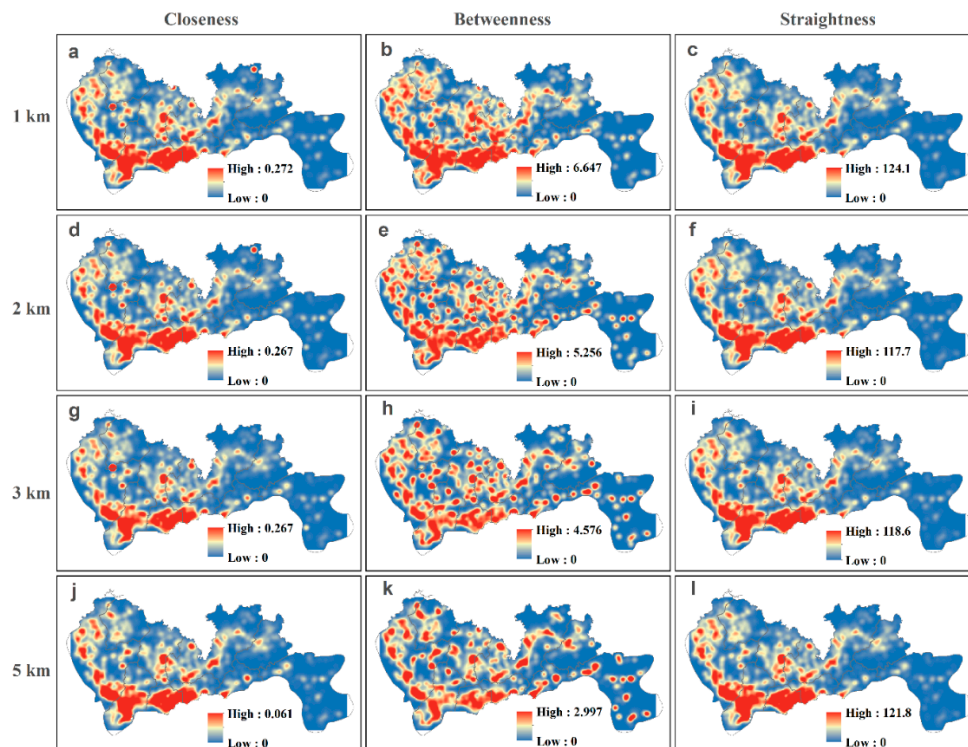
Figure 10. Spatial patterns of KDE of the local street centralities using searching radiuses of 1 km, 2 km, 3 km, and 5 km. The same vertical column shares the same centrality indicator: Closeness, Betweenness, and Straightness, from left to right, respectively. The same horizontal row shares the same searching radius: 1 km, 2 km, 3 km, and 5 km, from top to bottom, respectively.

Table 2. Pearson's *r* between local street centralities and land use intensities in the 1 km grid.

| Centralities	Comm [#]	Publ	Resi
Global C^C [##]	0.675 **	0.706 **	**0.592 ****
Local C^C_{1km}	**0.698 ****	**0.734 ****	0.541 **
Local C^C_{2km}	0.654 **	0.688 **	0.501 **
Local C^C_{3km}	0.597 **	0.629 **	0.452 **
Local C^C_{5km}	0.316 **	0.344 **	0.255 **
Global C^B	**0.405 ****	**0.413 ****	**0.433 ****
Local C^B_{1km}	0.296 **	0.325 **	0.264 **
Local C^B_{2km}	0.248 **	0.272 **	0.232 **
Local C^B_{3km}	0.215 **	0.239 **	0.201 **
Local C^B_{5km}	0.195 **	0.223 **	0.169 **
Global C^S	0.669 **	0.703 **	0.549 **
Local C^S_{1km}	0.733 **	0.771 **	0.563 **
Local C^S_{2km}	0.740 **	0.779 **	0.563 **
Local C^S_{3km}	0.744 **	0.783 **	0.565 **
Local C^S_{5km}	**0.747 ****	**0.785 ****	**0.569 ****

[#] Comm, Publ, and Resi mean commercial land, public service land, and residential land, respectively.
[##] Global centralities are also included for the convenience of comparison. ** $p < 0.01$.

5.2. Effect of Statistical Units

To test the impact of the different statistical units on the correlation between the street centralities and land use intensities, we summarized the street centralities and land use intensities using the Shenzhen subdistrict administrative units (census blocks). The spatial distributions of the street centralities and land use intensities at the census block level are shown in Figure 11. We only calculated the linear correlation between the street centralities and urban land use intensities under the optimal scales, which are presented in Table 3. Dapeng District is excluded from the correlation analysis for consistency, resulting in 58 census blocks in total.

The street centralities in the census blocks show an apparent concentration of high centralities in the core area (blue ellipses) in Figure 11a,c,e. The high intensities of commercial land and public service land are also concentrated in the core urban area (Figure 11b,d). However, for residential land, the Longhua and Minzhi blocks have high intensities, which are away from the core urban area (Figure 11f). Urban land intensities in Nanshan Disctrict (red circles), the high-technology zone, are relatively low compared to the Futian and Luohu districts, the initial special economic zones. The results of the correlation analysis show that the street centralities and urban land use intensities at the subdistrict level have a higher Pearson's r compared with that in the 1 km grid (Tables 2 and 3). The subdistricts that have a larger scale than the 1 km grid and can eliminate local noise, resulting in a higher degree of correlation.
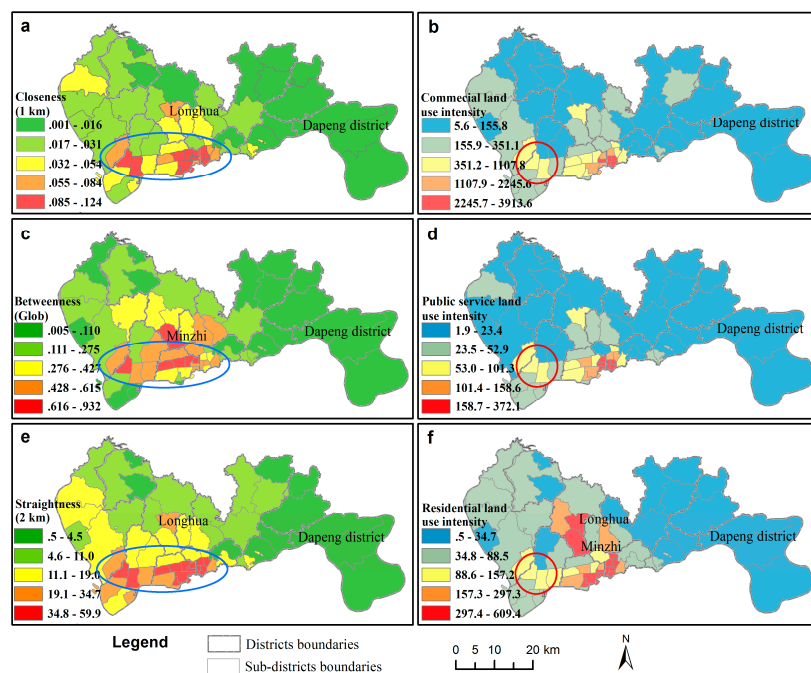
Figure 11. Spatial distributions of street centralities and land use intensities at the subdistrict level (census block) in Shenzhen City. (**a**) Closeness at 1 km searching radius, (**b**) Commercial land use intensity, (**c**) Global Betweenness, (**d**) Public service land use intensity, (**e**) Straightness at 2 km searching radius, (**f**) Residential land use intensity.

Table 3. Pearson's r between street centralities and land use intensities at the subdistrict level (census block) (N = 58).

Centralities	Comm [#]	Publ	Resi
Local C^C_{1km}	0.794 **	0.849 **	0.749 **
Global C^B	0.518 **	0.573 **	0.521 **
Local C^S_{5km}	0.819 **	0.872 **	0.753 **

[#] Comm, Publ, and Resi represent commercial land, public service land, and residential land, respectively.
** $p < 0.01$.

6. Conclusions

Urban land use structure and transport systems mutually interact. Previous studies on the interrelationships between street centralities and land use intensities relied on land cover data, neglecting the social functions of urban land use. Taking Shenzhen City as a case study, this study contributed to distinguishing the different types of urban land use using reclassified points of interest (POI) data and investigating their varying correlations with three street centralities (closeness, betweenness, and straightness). The high values of the global closeness and straightness centralities are concentrated in the urban core areas, while the high values of the global betweenness centralities highlight the backbone of the road network. As the searching radius increases, the spatial patterns of the local centralities are more similar to the global centralities, showing a transformation of local characteristics to overall features. The results of our correlation analysis show a general strong correlation between urban land intensities and street centralities. Specifically, commercial land and public service land are more correlated with street centralities than residential land, because the spatial distribution of residential land is relatively scattered compared to the other two types of urban land use. We also found that the closeness and straightness centralities have stronger abilities in measuring locational advantages than the betweenness centrality. The statistical units can affect the correlation between the street centralities and the land use intensities, and they are more correlated in a larger scale unit because of their reduced noise and ignored extraneous details. The analysis of the spatial patterns of street centralities and urban land use intensities, as well as their interdependence can help the implementation of urban land use planning and transportation planning.

This study uses POI data to characterize the different types of urban land use. However, the results are not verified by the determined data, which may reduce the feasibility of the result. Secondly, Shenzhen City is adjacent to Dongguan City and Huizhou City, and the residents of the three cities commute between each other frequently, especially at the junction of Shenzhen and Dongguan. This study only obtained the street network within the administrative boundaries of Shenzhen, resulting in a bias for the street centralities calculation at the edge of the city boundary, also known as the "edge effect" [42]. Finally, we only tested correlations between the street centralities and land use intensities and their variations. Their spatial distributions and interrelationships between them are complex, which can be influenced by regulation, history, as well as many other factors [21]. Further studies could help explain the mechanism of interdependence between urban land use and transportation.

Author Contributions: S.W. and G.X. conceived the experiments, analyzed the data, and wrote the paper. Q.G. reviewed and provided comments for revisions.

Conflicts of Interest: The authors declare no conflict of interest.

References

1. Badoe, D.A.; Miller, E.J. Transportation-land-use interaction: Empirical findings in North America, and their implications for modeling. *Transp. Res. Part D* **2000**, *5*, 235–263. [CrossRef]
2. Cao, X. Land use and transportation in China. *Transp. Res. Part D* **2017**, *52*, 423–427. [CrossRef]
3. Wang, Y.; Monzon, A.; Ciommo, F.D. Assessing the accessibility impact of transport policy by a land-use and transport interaction model—The case of Madrid. *Comput. Environ. Urban Syst.* **2015**, *49*, 126–135. [CrossRef]
4. Hansen, W.G. How accessibility shapes land use. *J. Am. Inst. Plan.* **1959**, *25*, 73–76. [CrossRef]
5. Sultana, S. Transportation and land use. In *International Encyclopedia of Geography*; John Wiley & Sons, Ltd.: New York, NY, USA, 2016.
6. Van Wee, B. Evaluating the impact of land use on travel behaviour: The environment versus accessibility. *J. Transp. Geogr.* **2011**, *19*, 1530–1533. [CrossRef]
7. Lee, M.; Barbosa, H.; Youn, H.; Holme, P.; Ghoshal, G. Morphology of travel routes and the organization of cities. *Nat. Commun.* **2017**, *8*, 2229. [CrossRef] [PubMed]

8. Jaarsma, C.F. Approaches for the planning of rural road networks according to sustainable land use planning. *Landsc. Urban Plan.* **1997**, *39*, 47–54. [CrossRef]

9. Shen, Y.; Karimi, K. The economic value of streets: Mix-scale spatio-functional interaction and housing price patterns. *Appl. Geogr.* **2017**, *79*, 187–202. [CrossRef]

10. Van Oort, F.; Burger, M.; Raspe, O. On the economic foundation of the urban network paradigm: Spatial integration, functional integration and economic complementarities within the Dutch Randstad. *Urban Stud.* **2010**, *47*, 725–748. [CrossRef]

11. Lin, J.; Ban, Y. Comparative analysis on topological structures of urban street networks. *ISPRS Int. J. Geo-Inf.* **2017**, *6*, 295.

12. Porta, S.; Crucitti, P.; Latora, V. The network analysis of urban streets: A dual approach. *Physica A* **2006**, *369*, 853–866. [CrossRef]

13. Porta, S.; Crucitti, P.; Latora, V. The network analysis of urban streets: A primal approach. *Environ. Plan. B* **2006**, *33*, 705–725. [CrossRef]

14. Crucitti, P.; Latora, V.; Porta, S. Centrality measures in spatial networks of urban streets. *Phys. Rev. E Stat. Nonlinear Soft Matter Phys.* **2006**, *73*, 036125. [CrossRef] [PubMed]

15. Crucitti, P.; Latora, V.; Porta, S. Centrality in networks of urban streets. *Chaos* **2006**, *16*, 015113. [CrossRef] [PubMed]

16. Wang, F.; Antipova, A.; Porta, S. Street centrality and land use intensity in Baton rouge, Louisiana. *J. Transp. Geogr.* **2011**, *19*, 285–293. [CrossRef]

17. Porta, S.; Strano, E.; Iacoviello, V.; Messora, R.; Latora, V.; Cardillo, A.; Wang, F.H.; Scellato, S. Street centrality and densities of retail and services in Bologna, Italy. *Environ. Plan. B* **2009**, *36*, 450–465. [CrossRef]

18. Porta, S.; Latora, V.; Wang, F.; Rueda, S.; Strano, E.; Scellato, S.; Cardillo, A.; Belli, E.; Càrdenas, F.; Cormenzana, B. Street centrality and the location of economic activities in Barcelona. *Urban Stud.* **2012**, *49*, 1471–1488. [CrossRef]

19. Wang, F.; Chen, C.; Xiu, C.; Zhang, P. Location analysis of retail stores in Changchun, China: A street centrality perspective. *Cities* **2014**, *41*, 54–63. [CrossRef]

20. Rui, Y.; Ban, Y. Exploring the relationship between street centrality and land use in Stockholm. *Int. J. Geogr. Inf. Sci.* **2014**, *28*, 1425–1438. [CrossRef]

21. Chaudhuri, G.; Clarke, K.C. On the spatiotemporal dynamics of the coupling between land use and road networks: Does political history matter? *Environ. Plan. B* **2015**, *42*, 133–156. [CrossRef]

22. Pei, T.; Sobolevsky, S.; Ratti, C.; Shaw, S.-L.; Li, T.; Zhou, C. A new insight into land use classification based on aggregated mobile phone data. *J. Geogr. Inf. Sci.* **2014**, *28*, 1988–2007. [CrossRef]

23. Zhou, M.; Yue, Y.; Li, Q.; Wang, D. Portraying temporal dynamics of urban spatial divisions with mobile phone positioning data: A complex network approach. *ISPRS Int. J. Geo-Inf.* **2016**, *5*, 240. [CrossRef]

24. Huang, B.; Zhao, B.; Song, Y. Urban land-use mapping using a deep convolutional neural network with high spatial resolution multispectral remote sensing imagery. *Remote Sens. Environ.* **2018**, *214*, 73–86. [CrossRef]

25. Yao, Y.; Li, X.; Liu, X.; Liu, P.; Liang, Z.; Zhang, J.; Mai, K. Sensing spatial distribution of urban land use by integrating points-of-interest and Google word2vec model. *J. Geogr. Inf. Sci.* **2016**, *31*, 825–848. [CrossRef]

26. Jiang, S.; Alves, A.; Rodrigues, F.; Ferreira, J.; Pereira, F.C. Mining point-of-interest data from social networks for urban land use classification and disaggregation. *Comput. Environ. Urban Syst.* **2015**, *53*, 36–46. [CrossRef]

27. Liu, X.; Long, Y. Automated identification and characterization of parcels with openstreetmap and points of interest. *Environ. Plan. B* **2015**, *43*, 341–360. [CrossRef]

28. Gao, S.; Janowicz, K.; Couclelis, H. Extracting urban functional regions from points of interest and human activities on location-based social networks. *Trans. GIS* **2017**, *21*, 446–467. [CrossRef]

29. Shen, Y.; Karimi, K. Urban function connectivity: Characterisation of functional urban streets with social media check-in data. *Cities* **2016**, *55*, 9–21. [CrossRef]

30. Yuan, J.; Zheng, Y.; Xie, X. Discovering Regions of Different Functions in a City Using Human Mobility and POIs. In Proceedings of the 18th ACM SIGKDD International Conference on Knowledge Discovery and Data Mining, Beijing, China, 12–16 August 2012; ACM: New York, NY, USA, 2012; pp. 186–194.

31. Wang, Y.; Gu, Y.; Dou, M.; Qiao, M. Using spatial semantics and interactions to identify urban functional regions. *ISPRS Int. J. Geo-Inf.* **2018**, *7*, 130. [CrossRef]

32. Yue, Y.; Zhuang, Y.; Yeh, A.G.O.; Xie, J.-Y.; Ma, C.-L.; Li, Q.-Q. Measurements of POI-based mixed use and their relationships with neighbourhood vibrancy. *J. Geogr. Inf. Sci.* **2016**, *31*, 658–675. [CrossRef]

33. Beruea of Statistics of Shenzhen. Statistical Communique of Shenzhen on Economic and Social Development in 2016. 2017. Available online: http://www.sz.gov.cn/cn/xxgk/zfxxgj/tjsj/tjgb/201705/t20170502_6199402.htm (accessed on 20 October 2018). (In Chinese)

34. Yao, Y.; Liu, X.; Li, X.; Liu, P.; Hong, Y.; Zhang, Y.; Mai, K. Simulating urban land-use changes at a large scale by integrating dynamic land parcel subdivision and vector-based cellular automata. *J. Geogr. Inf. Sci.* **2017**, *31*, 2452–2479. [CrossRef]

35. Tu, W.; Cao, J.; Yue, Y.; Shaw, S.-L.; Zhou, M.; Wang, Z.; Chang, X.; Xu, Y.; Li, Q. Coupling mobile phone and social media data: A new approach to understanding urban functions and diurnal patterns. *J. Geogr. Inf. Sci.* **2017**, *31*, 2331–2358. [CrossRef]

36. Haklay, M.; Weber, P. Openstreetmap: User-generated street maps. *IEEE Pervasive Comput.* **2008**, *7*, 12–18. [CrossRef]

37. Haklay, M. How good is volunteered geographical information? A comparative study of openstreetmap and ordnance survey datasets. *Environ. Plan. B* **2010**, *37*, 682–703. [CrossRef]

38. Boeing, G. Osmnx: New methods for acquiring, constructing, analyzing, and visualizing complex street networks. *Comput. Environ. Urban Syst.* **2017**, *65*, 126–139. [CrossRef]

39. Grippa, T.; Georganos, S.; Zarougui, S.; Bognounou, P.; Diboulo, E.; Forget, Y.; Lennert, M.; Vanhuysse, S.; Mboga, N.; Wolff, E. Mapping urban land use at street block level using openstreetmap, remote sensing data, and spatial metrics. *ISPRS Int. J. Geo-Inf.* **2018**, *7*, 246. [CrossRef]

40. Hacar, M.; Kılıç, B.; Şahbaz, K. Analyzing openstreetmap road data and characterizing the behavior of contributors in Ankara, Turkey. *ISPRS Int. J. Geo-Inf.* **2018**, *7*, 400. [CrossRef]

41. Sevtsuk, A.; Mekonnen, M. Urban network analysis. A new toolbox for arcgis. *Revue Int. Géomat.* **2012**, *22*, 287–305. [CrossRef]

42. Gil, J. Street network analysis "edge effects": Examining the sensitivity of centrality measures to boundary conditions. *Environ. Plan. B* **2016**, *44*, 819–836. [CrossRef]